Journal of Electroanalytical Chemistry 967 (2024) 118467

Contents lists available at ScienceDirect

Journal of Electroanalytical Chemistry

journal homepage: www.elsevier.com/locate/jelechem

Water-soluble biowaste gum binders for natural graphite anode for lithium-ion batteries

Joon Ha Chang [a,1], Min Wook Pin [b,1], Lawrence Robert Msalilwa [c,1], Sung Ho Shin [d], Chulwoong Han [e,f], Hyunung Yu [g], Zubair Ahmed Chandio [c], Vinod V.T. Padil [h,*], Youngjin Kim [i,*], Jun Young Cheong [c,j,*]

[a] LiB Materials Research Group, Secondary Battery Materials Research Laboratory, Research Institute of Industrial Science and Technology (RIST), 67 Cheongam-ro, Pohang 37673, Republic of Korea
[b] Industrial Materials R&D Group, Korea Institute of Industrial Technology, Incheon 21999, Republic of Korea
[c] Bavarian Center for Battery Technology (BayBatt) and Department of Chemistry, University of Bayreuth, Universitätsstraße 30, 95447 Bayreuth, Germany
[d] Jilli Hall, Korea Advanced Institute of Science and Technology, 193 Munji-ro, Yuseong-gu, Daejeon 34051, Republic of Korea
[e] Research Institute of Intelligent Manufacturing & Materials Technology, Korea Institute of Industrial Technology, 156, Gaetbeol-ro, Yeonsu-gu, Incheon 21999, Republic of Korea
[f] Materials Science and Engineering, Inha University, 100 Inha-ro, Michuhol-gu, Incheon 22212, Republic of Korea
[g] Advanced Instrumentation Institute, Korea Research Institute of Standards and Science, Daejeon 34113, Republic of Korea
[h] Amrita School for Sustainable Futures (ASF), Amrita Vishwa Vidyapeetham, Amritapuri, Kollam 690525, Kerala, India
[i] Department of Materials Science and Engineering, Kangwon National University, Chuncheon 24341, Republic of Korea
[j] James Watt School of Engineering, University of Glasgow, Glasgow G12 8QQ, UK

ARTICLE INFO

Keywords:
Biowaste
Water-soluble
Binder
Natural graphite
Anode

ABSTRACT

Anode materials for lithium-ion batteries (LIBs) are crucial, as lithium insertion takes place in the anode during the charging process. Also, it is rational to replace the conventional polyvinylidene fluoride (PVdF) with a water-soluble binder because the former employs *N*-Methyl-2-pyrrolidone, which is environmentally harmful. To address the problem, we fabricated natural graphite (NG)-based anodes with water-soluble biowaste (W-SB) binders from the gum of the tree *Cochlospermum gossypium* and PVdF. Both of the electrodes were fabricated using 10 wt% of binder and were evaluated for their electrochemical performance. The NG-W-SB electrode showed good mechanical properties and maintained structural integrity after cycling, this promoted low charge transfer resistance on the electrode. NG-W-SB-based electrode showed high current peaks in the 1st cycle being an indication of enhanced electrochemical performance, unlike the NG-PVdF electrode which showed slightly low peaks. NG-W-SB maintained a higher stable capacity retention up to 360 cycles, whereas NG-PVdF had a capacity degradation after 200 cycles indicating a low capacity retention until the end of the cycle. Generally, W-SB binders showed highly enhanced cycling retention characteristics, comparable rate capabilities, and lower electrode resistance, which opened a new avenue for adopting biowaste (gum) as a functional water-soluble binder for LIBs applications.

1. Introduction

Since its commercialization in 1991 [1–3], lithium-ion battery (LIBs) technology has seen gradual advancements, and today it has been applied in the field of the emerging technology of portable electronics and now electric vehicles [1,3–7] owing to their captivating electrochemical properties [8,9]. Recently, they were awarded "Nobel Prize in Chemistry" (2019) [10,11]. In particular, anode materials are quite critical as they accept lithium-ion during the charging process. Graphite is consistently the first choice and most popular anode material and is extensively used, due to its reversible lithium-ion intercalation [12], pleasing electrochemical characteristics, and low-cost fabrication

* Corresponding authors at: Bavarian Center for Battery Technology (BayBatt) and Department of Chemistry, University of Bayreuth, Universitätsstraße 30, 95447 Bayreuth, Germany (J.Y. Cheong).
E-mail addresses: vinodvtp@am.amrita.edu (V.V.T. Padil), ykim@kangwon.ac.kr (Y. Kim), JunYoung.Cheong@glasgow.ac.uk (J.Y. Cheong).
[1] These authors contributed equally to this work.

https://doi.org/10.1016/j.jelechem.2024.118467
Received 23 April 2024; Received in revised form 17 June 2024; Accepted 25 June 2024
Available online 28 June 2024

[7,12–14]. Natural graphite (NG) has attracted great attention for reducing CO_2 emission [15], and both the cycling stability and rate capabilities are important parameters for NG anode, which have been previously reported [16–18]. For any electrodes, the adhesion between active materials, conductive agents, and current collectors is important in achieving electrode stability and stable electrochemical performance [8,9,12,19,20] and in fact, this has been made possible by the use of binders. Recently, novel concepts of binders have been reported including hyperbranched networks [21–23] crosslinking [24–26] and conductive binders [27,28]. On the other hand, numerous natural binders, such as agar-agar (AA), xanthan gum (XG), carrageenan (CAR), guar gum (GG), sodium alginate (SA) [2], sodium carboxymethyl cellulose (Na-CMC) [2,29] and Tamarind Kernel Powder (TKP) [13] have already been studied and reported to have various advantages such as water solubility, easy availability, and environmental friendliness which makes them suitable for use as graphite binders.

Polymer binders such as polyvinylidene fluoride (PVdF) is the dominant and most commonly used binder to prepare the traditional graphite anodes [8,30,31] however currently, the existing PVdF-based binder system has failed to meet the requirements of emerging high-capacity active materials because it is incompatible with lithiated graphite at high temperatures and partially decomposes during electrochemical cycling [12]. Furthermore, conventional polyvinylidene fluoride (PVdF) based electrode needs to be dissolved in 1-Methyl-2-pyrrolidinone (NMP) as an organic solvent, which is toxic and not environmentally friendly [32,33]. However, in spite of having plenty of other natural gums, less effort has been devoted to exploring novel binders from natural materials to boost battery performance [30,34]. Researchers have recently dedicated their efforts to investigating the usage of water-soluble binders as an alternative material to PVdF in the anode of lithium-ion batteries [7,12]. Therefore, water-soluble binders (such as carboxymethyl cellulose) have attracted much attention [35–37] because they are usually deemed as green binders, naturally available, and easy to disperse in water. They are also effective in promoting cathode/anode electrochemical performances, compared with the PVdF-based binders [12]. The water-soluble binders, renowned for their polar functional groups (carboxyl and hydroxyl groups) and cross-linked structure, are highly regarded for their exceptional chemical bonding properties [38–41]. Their distinctive combination of polar functional groups and cross-linked structure makes them an attractive option for establishing robust and long-lasting chemical bonds in a number of electrode materials. In recent studies, considerable attention has been devoted to exploring other biowaste binders that exhibit similar chemical structures and properties as binders [42–45].

In this work, we have employed biowaste-based gums and made a water-soluble biowaste (W-SB) binder solution for the NG anode, which has major advantages over the conventional water-soluble polymer in terms of cost and abundance (produced largely over the globe). In contrast to chemically synthesized polymer, these biowastes are produced naturally on a yearly basis, which are more eco-friendly and environmentally benign. This is the initial work on employing biowaste material (gum from the tree) as an aqueous binder for NG, as most gum-based binder work was carried out for Si anode [41,46–48] and/or other kinds of graphite/carbon [2,36]. Tree gum as a biowaste material was rarely utilized as a binder for the NG, let alone the deacetylated gum-based binder for NG. NG is still one of the most conventional anode materials that are used in commercial batteries because of its low cost and abundance. Sustainable utilization of biowastes has been tried in various applications [49–51], which is in agreement with this work. W-SB binders were compared with PVdF binders, and they exhibited excellent electrochemical performance.

2. Experimental details

2.1. Materials

The biowaste is a gum extracted from the *Cochlospermum gossypium* tree. Other materials such as sodium hydroxide (NaOH, reagent grade, ≥ 98 %, pellets (anhydrous)), and hydrochloric acid (HCl, ACS reagent, 37 %) were used to remove the acetyl group during the extraction of biowaste (gum). The NG anode powder was purchased and used as active material in the working electrodes. Polyvinylidene difluoride (PVdF) was utilized as a binder for comparative purposes and 1-Methyl-2-pyrrolidinone (NMP, anhydrous) a solvent to dissolve PVdF. All the materials were purchased from Sigma Aldrich.

2.2. W-SB preparation and electrode fabrication

W-SB binder was made by the deacetylation process of the biowaste (gum) [52,53]. The process involved the removal of acetyl groups of the biowaste, which was characterized by soaking with NaOH, neutralization process, dialysis, and freeze-drying. The biowaste powder (1 g/L) was mixed with 1 M NaOH aqueous solution (3:1 in vol. in deionized water) and it was stirred with a magnetic bar for 30 min at room temperature. The solution was then neutralized with 1 M HCl solution. The deacetylated kondagogu gum (KG) was extensively dialyzed to eliminate the remaining salts. Filtration of impurities took place through a sintered glass funnel No. G-2 followed by the glass funnel No. G-4. The final solution was freeze-dried and stored for further use. For the control sample, PVdF was dissolved in NMP solvent as the binder solution. The electrode was fabricated by mixing an active material (NG), conductive agent, and binder (W-SB or PVdF) at a weight ratio of 8:1:1 respectively. Appropriate amounts of water (for the W-SB) or NMP (for PVdF) were respectively added as solvents to obtain a uniform slurry, which was cast onto a copper foil and dried under a vacuum oven until the solvent vaporized fully.

2.3. Cell assembly process

Both the anode containing PVdF binder and W-SB binder were assembled with a separator and lithium metal in a half-coin cell. The active mass loading was about 1.1 mg cm^{-2}. A Celgard 2325, and 1.0 M of lithium hexafluorophosphate ($LiPF_6$) dissolved in a mixed solvent of ethylene carbonate/diethylene carbonate (EC/DEC, v/v = 1:1), were used as a separator and electrolyte respectively. Coin cells were assembled in a dry room, where, in all cases the metallic lithium discs were used as counter electrodes. The cells were aged for 24 hand were subjected to undergo electrochemical cell testing.

2.4. Characterization

Morphological aspects of NG powders were examined by Scanning Electron Microscope (SEM, JEOL 7100F, JEOL) at an accelerating voltage of 5 kV. The chemical and structural properties of NG powder & W-SB binder were analyzed by Fourier Transform Infrared Spectroscopy (FTIR, Nicolet 6700, Thermo Fisher Scientific) and Raman Spectroscopy (DXR, Thermo Fisher Scientific). Mechanical properties were further examined by nano-indentation test with the load range of 0 to 1.0 mN using the harness measurement system (FischerScope HM2000, Hermut Fischer). Cyclic Voltammetry (CV) analysis was employed at a scan rate of 0.1 mV s−1 using a cell tester (Arbin 32 Channels, ± 5 V, 200 mA, 2 x Gamry 1010E, Aux Chassis). Galvanostatic voltage profile, cycle retention tests, and rate capabilities were examined in a voltage window of 0.005–2.0 V. Electrochemical impedance spectroscopy was carried out using the impedance tester (Biologic). Impedance was recorded at the open circuit voltage in the frequency range from 0.1 Hz to 1 MHz with 5 mV of Vrms. The formation process was extant before the cycle retention test. Ex situ SEM analysis was carried out on the anode after cycling.

3. Results and discussion

The schematic illustration of the W-SB binder preparation, anode slurry fabrication, and electrode finalization are presented in Fig. 1a. The biowaste gum from the tree becomes soluble in water after the deacetylation process, which led to the removal of acetyl groups (Fig. S1). Then, the binder solution is mixed with the NG anode to produce an anode slurry, which can be cast onto the Cu current collector. SEM image of NG powder (Fig. 1b) shows typical NG anode morphology, characterized by micron-scale particles with high tap density (particle sizes mostly ranging from 5 to 20 μm). The Raman analysis was carried out to analyze the degree of structural ordering of NG materials as shown in Fig. 1c. Raman spectrum exhibited a predominant peak of the G band with a D band shoulder, to show less defect present compared with synthetic graphite. The two distinct peaks of the D band (at ~1350 cm^{-1}) and G band (at ~1580 cm^{-1}) was also reported with similar observation comparing the NG and synthetic graphite materials [54,55]. To understand the effect of deacetylation process on the W-SB material, the presence of acetyl groups (Peaks at 1731 cm^{-1} and 1249 cm^{-1}) was verified through FTIR analysis (Fig. 2). After the deacetylation process, the peaks ascribed to the acetyl groups either decreased or disappeared [38], which shows the effective deaccetylation that changed the chemical bonding of the W-SB material.

The loading and unloading curves of nano indentation tests for NG-W-SB and NG-PVdF are shown in Fig. 3. The NG-W-SB electrode unloading curves terminated at depths between 0.6 and 1.0 μm (Fig. 3a), while the NG-PVdF electrode terminated at depths between 0.9 and 1.5 μm (Fig. 3b), which means that the residual indentations in the NG-PVdF electrode are deeper than those in the NG-W-SB electrode area. The NG-PVdF-based electrode underwent a more severe plastic deformation than the NG-W-SB-based electrode after indentation tests. Based on the nano-indentation test and calculated average hardness/Young's modulus (Fig. 4a and b), the replacement of PVdF with W-SB binder led to significantly improved mechanical properties. Normally, the adhesion strength is higher when more binder content is used [8,19,56]. For the same weight ratio used for the binders, the W-SB binder was observed to report higher values of hardness/Young's modulus which could be attributed to the increased adhesion capability of the binder. Other water-soluble binders such as PAA, alginate, and CMC also have better adhesion strength than PVdF due to the strong hydrogen bond it contains [30] as in the W-SB binder.

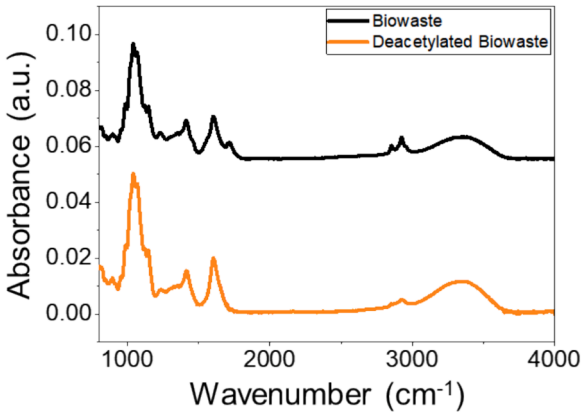

Fig. 2. FTIR analysis of W-SB material before and after the deacetylation process.

To investigate the role that W-SB binder plays that distincts it from the PVdF binder, both the internal resistance of the cell and the structural integrity of the electrode were examined by electrochemical impedance spectroscopy (EIS) and ex-situ SEM. The electrochemical cells composed of NG-PVdF and NG-W-SB electrodes after cycling were analyzed for impedance test, and Nyquist plots (Fig. 5a) suggest smaller charge transfer resistance of the electrochemical cell for W-SB binder compared with PVdF binder. Using the equivalent circuit (Fig. S1) model to fit the Nyquist plots, the values for R_s, R_{SEI}, and R_{CT} were determined and compared for NG-PVdF and NG-W-SB (expressed in Table S1). The R_{SEI} and R_{CT} values for NG-W-SB are 3.18 and 30.80 Ohm, while those of

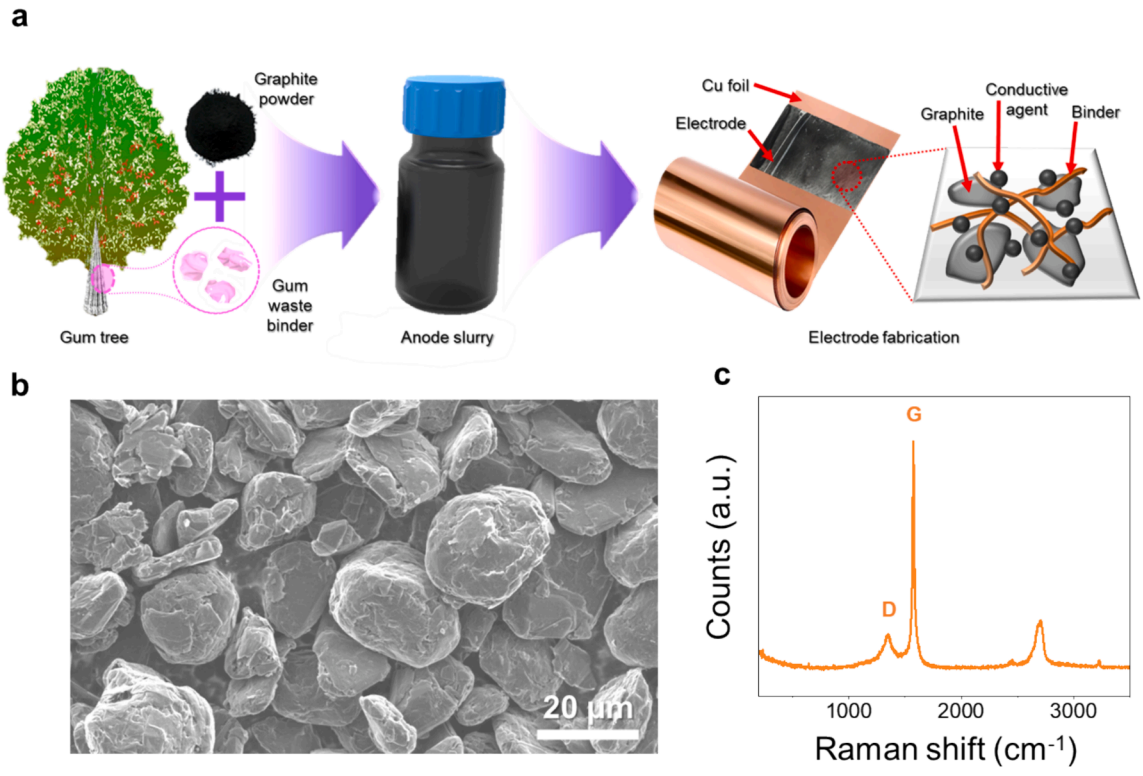

Fig. 1. (a) Schematic illustration of fabrication steps of W-SB binder. (b) SEM image of NG anode. (c) Raman spectrum of NG anode.

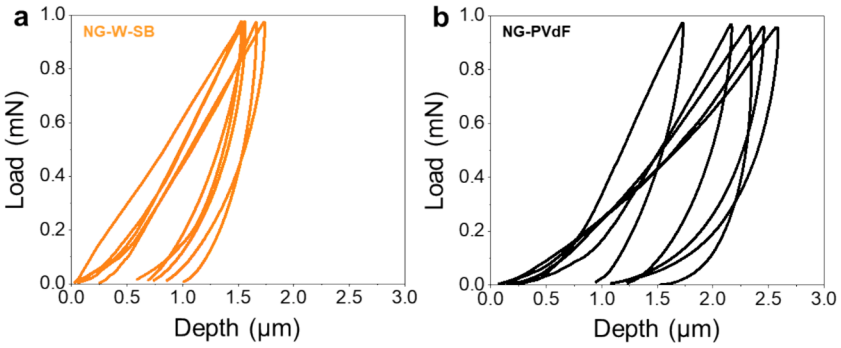

Fig. 3. Nano-indentation profiles of (a) NG-W-SB and (b) NG-PVdF.

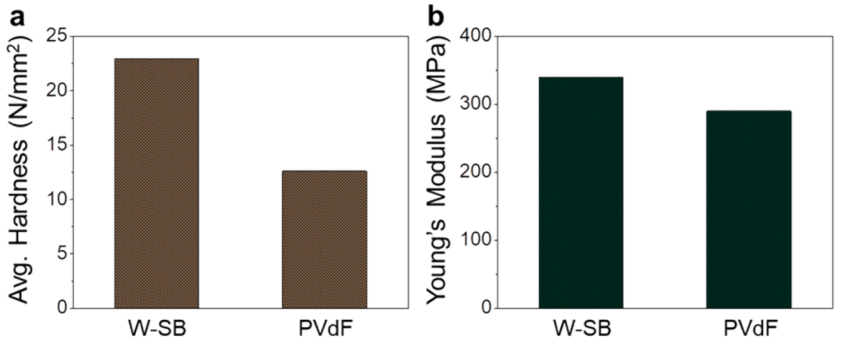

Fig. 4. (a) Average hardness (N/mm^2) and (b) Young's modulus of NG-W-SB and NG-PVdF electrode.

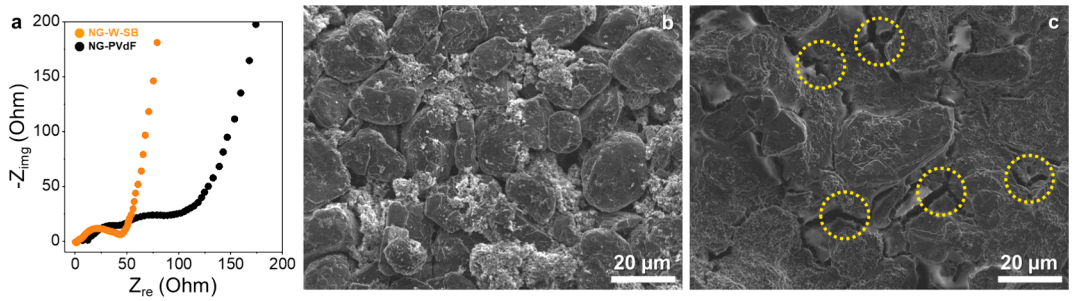

Fig. 5. (a) Nyquist plot of NG-W-SB and NG-PVdF after cycling. *Ex situ* SEM image of (b) NG-W-SB and (c) NG-PVdF (yellow dotted circles for cracks) after cycling.

NG-PVdF are 2.95 and 78.96 Ohm. Although R_{SEI} values are comparable, the R_{CT} of NG-W-SB is significantly smaller than that of NG-PVdF, which is ascribed to the facile charge transport of the NG-W-SB cell. The electrochemical cells were disassembled and further probed for their structural integrity after cycling. When the morphology of the NG-W-SB electrode (Fig. 5b) and the NG-PVdF electrode (Fig. 5c) was examined after cycling, more structural integrity was observed for the NG anode with W-SB binder. The individual NG particles were present with a W-SB binder (similar to Fig. 1b), and they did not undergo much structural degradation and/or additional surface changes. However, for the PVdF binder, agglomeration of NG anode particles together with cracks in the electrode was seen due to a typical residual indentation in the electrode after cycling. The Nyquist plots and postmortem analysis correlate with each other. The resistance of NG-W-SB is lower than that of NG-PVdF because NG-W-SB shows enhanced structural integrity after cycling and as a result, electrical contact is still maintained. On the other hand, cracks are already apparent for NG-PVdF, which leads to the loss of electric contact and therefore it has higher resistance as well as rapid capacity fading. To summarize, both the resistance and structural integrity of the electrode significantly improved when the W-SB binder was used, which shows the possibility of employing it as an advanced binder system in combination with graphite anode.

The electrochemical analysis and performance of the NG anode with W-SB binder and PVdF binder were further compared and evaluated. Cyclic voltammetry (CV) analysis was carried out for the NG anode with PVdF binder (Fig. 6a) and W-SB binder (Fig. 6b) at a scan rate of 0.1 mV s^{-1}. The very broad peak at 0.6–0.7 V and a sharp peak at 0 V appear in the cathodic scan for both binders, ascribed to the formation of solid electrolyte interphase (SEI) layer [57] and lithium-ion intercalation [58]. The sharp peak at 0.25 V in the anodic scan is ascribed to the lithium-ion de-intercalation, matching a previous work [8,58]. It can be noted that lithiation and de-lithiation peaks for both electrodes are situated at nearly the same potential, there is no considerable potential shift in the redox peaks. Overall, both W-SB and PVdF binders exhibit comparable redox reactions with lithium-ion. Further notice is in the 1st cycle of CV that, PVdF-based electrode has lower current peaks compared with the W-SB-based electrode which showed an improved current peak. The lower and high current peaks for both electrodes might be ascribed to the sluggish formation of the SEI layer and the higher rate of lithiation in the NG matrix respectively. Generally, the improved current peak for NG-W-SB in the 1st cycle is the indication of enhanced electrochemical activity performance of the respective

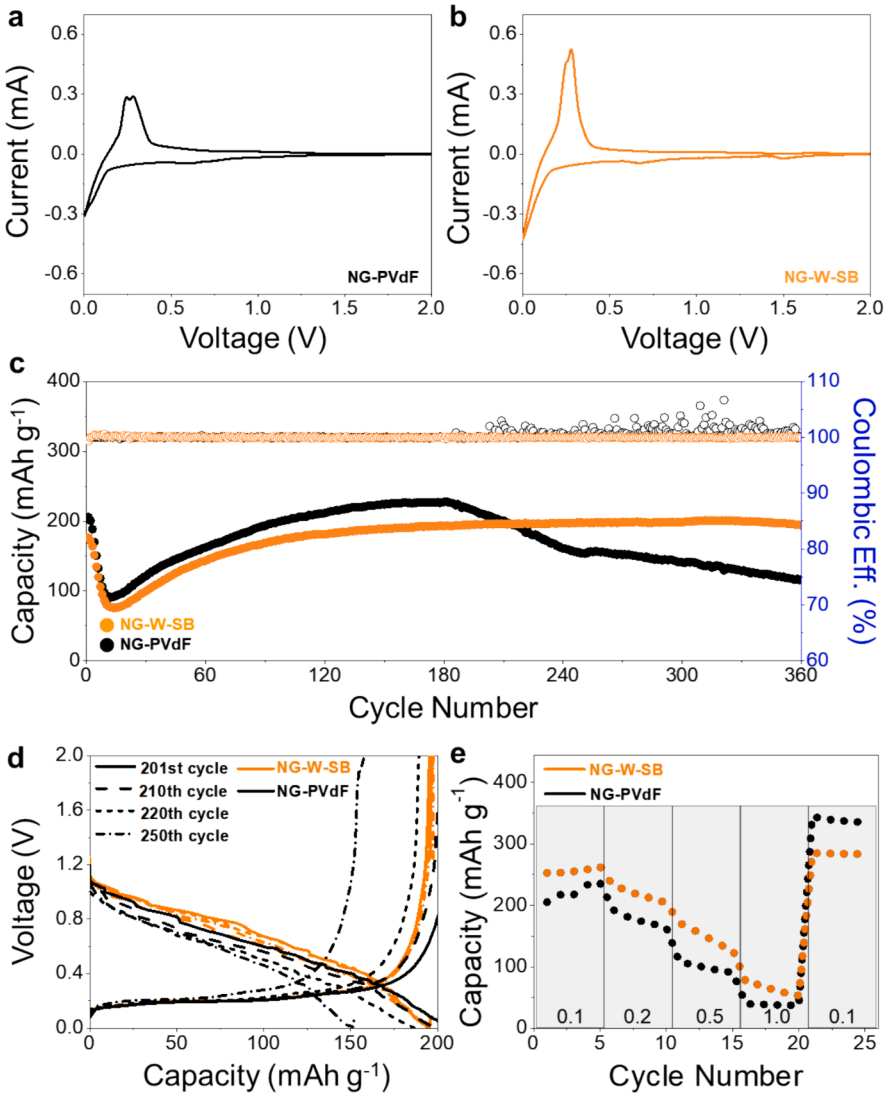

Fig. 6. CV curves of NG anode with (a) PVdF binder and (b) W-SB binder. (c) Cycling retention characteristics of NG-W-SB and NG-PVdF. (d) Charge and discharge profile of NG-W-SB and NG-PVdF electrode in the 201st, 210th, 220th, and 250th cycle. (e) Rate capabilities of NG anode with PVdF binder and W-SB binder (expressed in A g^{-1}).

electrodes compared with NG-PVdF.

The cycle stability of the NG-PVdF and NG-W-SB electrodes was tested at a current density of 0.5 A g^{-1}. Initially, the reversible capacity of the NG-PVdF electrode was slightly higher than that of the NG-W-SB electrode. Their capacity decreased and subsequent capacity increase took place (Fig. 6c), ascribed to the stabilization/activation process for graphite [59,60]. After 200 cycles, NG-PVdF starts undergoing capacity degradation indicating low capacity retention at the end of the cycle. On the other hand, NG-W-SB still maintains a higher stable capacity retention up to 360 cycles, which shows superior electrochemical performance. Additionally, some fluctuations in the coulombic efficiency of NG-PVdF take place, not present in NG-W-SB. Such fluctuations in the coulombic efficiency were observed elsewhere when the substantial capacity degradation takes place [16,61]. Based on the comparison of the rate capabilities and cycle retention characteristics, the W-SB binder leads to enhanced electrochemical performance. The overall electrochemical performance of NG-PVdF (control sample) is comparable and/or improved compared with that of the graphite-PVdF samples from the previously reported works [16–18], although many variables exist in assessing the electrochemical performance. To compare the capacity degradation phenomena that are prevalent for the NG-PVdF electrode, charge and discharge profile of NG-W-SB and NG-PVdF electrode in the 201st cycle, 210th cycle, 220th cycle, and 250th cycle are presented (Fig. 6d). In contrast to NG-W-SB that shows almost identical charge and discharge curves, the fluctuations of the charge and discharge curves are prominent for NG-PVdF electrode. More stable electrochemical performances are also observed in the rate capabilities test (Fig. 6e), where the capacity gradually increases for NG-PVdF whereas NG-W-SB already exhibits relatively higher capacity in the initial cycles. In rate capabilities at different current densities (from 0.1 to 1.0 A g^{-1}), the W-SB binder exhibits comparable rate capabilities compared with the PVdF binder. Furthermore, when the PVdF binder is used, the capacity relapses at the second 0.1 A g^{-1} from 1.0 A g^{-1}, it is not as constant as the W-SB binder. The slightly lower rate capability performance for PVdFPVdF-based electrode samples might resulted in result from limited lithium-ion distribution and high charge transfer resistance, and this is confirmed by EIS shown in Fig. 5a.

This work has shown a promising result obtained from the NG-W-SB electrode supporting other previous work performed in numerous water-soluble binders with graphite [2,9,13]. Based W-SB-based electrode showed slightly higher rate performance to concerning PVdF based electrode. It should be noted that although the overall electrochemical performance was relatively limited compared with the optimized anode design based on graphite, this is an initial work on comparing the role of

W-SB binder that is distinct from PVdF. On the other hand, although having inferior electrochemical performance compared with synthetic graphite, natural graphite offers advantages over synthetic graphite based on the lower cost and reducing CO_2 emissions [15,62] as the production of synthetic graphite is more expensive due to longer production time and requires more energy, emitting more CO_2 emissions. Through material and processing optimization, more enhanced electrochemical performance is expected in future studies. One challenge that needs to be resolved is to make sure that uniform properties are maintained within the binder solution that is produced in different time and season, so quality control is one important aspect that needs to be addressed.

4. Conclusion

In this work, we have successfully employed W-SB binders a naturally occurring material for the NG anode, which are environment-friendly, to be an alternative material to conventional PVdF binders for lithium-ion batteries. Electrochemical analyses and tests reveal the enhanced rate capabilities and cycling stability of the electrode with the W-SB binder. The introduction of the W-SB binder also led to structural integrity and decreased electrode resistance after cycling. Since graphite is still the most dominant anode material that is used in commercial battery, NG is chosen to further investigate the effect of employing W-SB binders on the anode and its electrochemical properties and performances. This is also attributed to the fact that NG is a good standard anode material that can initially be tested for the feasibility of a new binder type. The work shows the potential of employing a W-SB binder for prospective anode and cathode materials for LIBs and other next-generation energy storage systems in stationary or mobile device applications.

CRediT authorship contribution statement

Joon Ha Chang: Writing – review & editing, Writing – original draft, Investigation, Formal analysis, Data curation. **Min Wook Pin:** Writing – original draft, Methodology, Investigation, Formal analysis, Data curation. **Lawrence Robert Msalilwa:** Writing – review & editing, Writing – original draft, Validation. **Sung Ho Shin:** Writing – review & editing, Visualization, Software, Conceptualization. **Chulwoong Han:** Writing – review & editing, Writing – original draft, Formal analysis. **Hyunung Yu:** Methodology, Investigation. **Zubair Ahmed Chandio:** Writing – review & editing, Validation. **Vinod V.T. Padil:** Writing – review & editing, Writing – original draft, Supervision, Formal analysis, Conceptualization. **Youngjin Kim:** Writing – review & editing, Writing – original draft, Project administration, Formal analysis, Conceptualization. **Jun Young Cheong:** Writing – review & editing, Writing – original draft, Visualization, Validation, Supervision, Project administration, Methodology, Investigation, Funding acquisition, Data curation, Conceptualization.

Declaration of competing interest

The authors declare that they have no known competing financial interests or personal relationships that could have appeared to influence the work reported in this paper.

Acknowledgments

This work was supported by funding from Bavarian Center for Battery Technology (BayBatt), Bayerisch-Tschechische Hochschulagentur (BTHA) (BTHA-AP-2022-45, BTHA-AP-2023-5, BTHA-AP-2023-12, and BTHA-AP-2023-38), the University of Bayreuth-Deakin University Joint Ph.D. Program, Bayerische Forschungallianz (BayFOR) (BayIntAn_UBT_2023_84), BK21 program from National Research Foundation of Korea, Erasmus+ program from the European Union, Ministry of Education, Science and Technology as part of the Higher Education for Economic Transformation (HEET) Project (World Bank), Verband der Chemischen Industrie (Fonds der Chemischen Industrie, No. 661740), and collaboration project funding from Kangwon National University and LINC 3.0 Research Center. This work was also supported by the - Deutsche Forschungsgemeinschaft (DFG, individual project/project number: 533115776), AMRITA Seed Grant (Proposal ID: ASG2022104), Amrita University, India, and University of Glasgow Startup Fund. The authors would like to also thank Prof. Jeongsik Yun for detailed assistance in interpreting the impedance test results.

Appendix A. Supplementary data

Supplementary data to this article can be found online at https://doi.org/10.1016/j.jelechem.2024.118467.

References

[1] L. Rao, X. Jiao, C.Y. Yu, A. Schmidt, C. O'Meara, J. Seidt, J.R. Sayre, Y.M. Khalifa, J.H. Kim, ACS Appl. Mater. Interfaces 14 (1) (2022) 861–872.
[2] N. Cuesta, A. Ramos, I. Cameán, C. Antuña, A.B. García, Electrochim. Acta 155 (2015) 140–147.
[3] A. Ramos, I. Cameán, N. Cuesta, C. Antuña, A.B. García, Electrochim. Acta 187 (2016) 496–507.
[4] G. Harper, R. Sommerville, E. Kendrick, L. Driscoll, P. Slater, R. Stolkin, A. Walton, P. Christensen, O. Heidrich, S. Lambert, Nature 575 (7781) (2019) 75–86.
[5] A. Farmann, W. Waag, A. Marongiu, D.U. Sauer, J. Power Sources 281 (2015) 114–130.
[6] M. Winter, B. Barnett, K. Xu, Chem. Rev. 118 (23) (2018) 11433–11456.
[7] L. Ding, P. Bagul, L. Cui, S. Oswald, B. Pohle, R. Leones, D. Mikhailova, ACS Appl. Energy Mater. 6 (8) (2023) 4404–4412.
[8] N.J. Azaki, A. Ahmad, N.H. Hassan, M.A.A. Mohd Abdah, M.S. Su'ait, N. Ataollahi, T.K. Lee, ACS Appl. Polym. Mater. 5 (7) (2023) 4953–4965.
[9] P.S. Salini, S.V. Gopinadh, A. Kalpakasseri, B. John, M. Thelakkattu Devassy, A.C. S. Sustainable, Chem. Eng. 8 (10) (2020) 4003–4025.
[10] P.V. Kamat, ACS Energy Lett 4 (11) (2019) 2757–2759.
[11] Y.S. Hu, Y. Lu, ACS Energy Lett. (2019) 2689–2690.
[12] R.D. Lahiru Sandaruwan, R. Kuramoto, B. Wang, S. Ma, H. Wang, Langmuir 38 (29) (2022) 8934–8942.
[13] V.V. Narasimha Phanikumar, B.V. Appa Rao, K.V. Gobi, R. Gopalan, R. Prakash, ChemistrySelect 5 (3) (2020) 1199–1208.
[14] C. Capiglia, (2014).
[15] L. Zhao, B. Ding, X.Y. Qin, Z. Wang, W. Lv, Y.B. He, Q.H. Yang, F. Kang, Adv. Mater. 34 (18) (2022) 2106704.
[16] A. Gupta, R. Badam, A. Nag, T. Kaneko, N. Matsumi, ACS Appl. Energy Mater. 4 (3) (2021) 2231–2240.
[17] Z. Wang, G. Dang, Q. Zhang, J. Xie, Int. J. Electrochem. Sci. 12 (8) (2017) 7457–7468.
[18] Y. Wang, L. Zhang, Q. Qu, J. Zhang, H. Zheng, Electrochim. Acta 191 (2016) 70–80.
[19] B. Son, M.-H. Ryou, J. Choi, T. Lee, H.K. Yu, J.H. Kim, Y.M. Lee, ACS Appl. Mater. Interfaces 6 (1) (2014) 526–531.
[20] S. Sun, D. He, P. Li, Y. Liu, Q. Wan, Q. Tan, Z. Liu, F. An, G. Gong, X. Qu, J. Power Sources 454 (2020) 227907.
[21] Y.K. Jeong, T.W. Kwon, I. Lee, T.S. Kim, A. Coskun, J.W. Choi, Nano Lett. 14 (2) (2014) 864–870.
[22] F. Zeng, W. Wang, A. Wang, K. Yuan, Z. Jin, Y.S. Yang, ACS Appl. Mater. Interfaces 7 (47) (2015) 26257–26265.
[23] Y. Bie, J. Yang, X. Liu, J. Wang, Y. Nuli, W. Lu, ACS Appl. Mater. Interfaces 8 (5) (2016) 2899–2904.
[24] T.W. Kwon, Y.K. Jeong, E. Deniz, S.Y. AlQaradawi, J.W. Choi, A. Coskun, ACS Nano 9 (11) (2015) 11317–11324.
[25] B. Gendensuren, E.-S. Oh, J. Power Sources 384 (2018) 379–386.
[26] S. Lim, H. Chu, K. Lee, T. Yim, Y.J. Kim, J. Mun, T.H. Kim, ACS Appl. Mater. Interfaces 7 (42) (2015) 23545–23553.
[27] H. Zhao, A. Du, M. Ling, V. Battaglia, G. Liu, Electrochim. Acta 209 (2016) 159–162.
[28] N. Salem, M. Lavrisa, Y. Abu-Lebdeh, Energy Technol. 4 (2) (2016) 331–340.
[29] N. Lingappan, L. Kong, M. Pecht, Renew. Sustain. Energy Rev. 147 (2021) 111227.
[30] H. Chen, M. Ling, L. Hencz, H.Y. Ling, G. Li, Z. Lin, G. Liu, S. Zhang, Chem. Rev. 118 (18) (2018) 8936–8982.
[31] L. Li, T. Li, Y. Sha, C. Zhang, B. Ren, L. Zhang, S. Zhang, Ind. Eng. Chem. Res. 60 (48) (2021) 17399–17407.
[32] J. Chang, J. Zuo, L. Zhang, G.S. O'Brien, T.-S. Chung, J. Membr. Sci. 539 (2017) 295–304.
[33] D. Versaci, R. Nasi, U. Zubair, J. Amici, M. Sgroi, M. Dumitrescu, C. Francia, S. Bodoardo, N. Penazzi, J. Solid State Electrochem. 21 (2017) 3429–3435.
[34] Y. Bie, J. Yang, Y. Nuli, J. Wang, J. Mater. Chem. A 5 (5) (2017) 1919–1924.
[35] J.Y. Cheong, J.H. Chang, S.-H. Cho, J.-W. Jung, C. Kim, K.S. Dae, J.M. Yuk, I.-D. Kim, Electrochim. Acta 295 (2019) 7–13.

[36] F.M. Courtel, S. Niketic, D. Duguay, Y. Abu-Lebdeh, I.J. Davidson, J. Power Sources 196 (4) (2011) 2128–2134.
[37] C. Luo, L. Du, W. Wu, H. Xu, G. Zhang, S. Li, C. Wang, Z. Lu, Y. Deng, ACS Sustain. Chem. Eng. 6 (10) (2018) 12621–12629.
[38] V.T.P. Vinod, R.B. Sashidhar, Indian J. Nat. Prod. Resour. 1 (2010) 181–192.
[39] B. Reddy, H.-J. Ahn, J.-H. Ahn, G.-B. Cho, K.-K. Cho, J. Energy Storage 66 (2023) 107400.
[40] H.J. Chang, I.A. Rodríguez-Pérez, M. Fayette, N.L. Canfield, H. Pan, D. Choi, X. Li, D. Reed, Carbon Energy 3 (3) (2021) 473–481.
[41] Z. Wang, T. Huang, A. Yu, J. Power Sources 489 (2021) 229530.
[42] H. Moon, A. Innocenti, H. Liu, H. Zhang, M. Weil, M. Zarrabeitia, S. Passerini, ChemSusChem 16 (1) (2023) e202201713.
[43] C. Senthil, S.-S. Kim, H.Y. Jung, Nat. Commun. 13 (1) (2022) 145.
[44] Y.L. Chu, Y.C. Huang, Y.C. Tseng, C.C. Chang, H. Teng, B.H. Chen, J.S. Jan, J. Power Sources 552 (2022) 232205.
[45] T. Zhao, Y. Meng, H. Yin, K. Guo, R. Ji, G. Zhang, Y. Zhang, Chem. Phys. Lett. 742 (2020) 137145.
[46] J.W. Sturman, C.-H. Yim, Z. Karkar, E.A. Baranova, M. Toupin, Y. Abu-Lebdeh, J. Electrochem. Soc. 170 (2) (2023) 020534.
[47] X. Ren, T. Huang, A. Yu, Electrochem. Commun. 136 (2022) 107241.
[48] L. Qiu, Y. Shen, H. Fan, X. Yang, C. Wang, Int. J. Biol. Macromol. 115 (2018) 672–679.
[49] W.Y. Chia, K.W. Chew, C.F. Le, S.S. Lam, C.S.C. Chee, M.S.L. Ooi, P.L. Show, Environ. Pollut. 267 (2020) 115662.
[50] E. Sarlaki, A.M. Kermani, M.H. Kianmehr, K.A. Vakilian, H. Hosseinzadeh-Bandbafha, N.L. Ma, M. Aghbashlo, M. Tabatabaei, S.S. Lam, Environ. Pollut. 285 (2021) 117412.
[51] R.K. Ramakrishnan, S. Palanisamy, N.S. Sumitha, A.K.K. Padinjareveetil, S. Wacławek, T. Uyar, M. Černík, R.S. Varma, J.Y. Cheong, V. Vellora Thekkae Padil, ACS Sustain. Chem. Eng. 11 (19) (2023) 7344–7356.
[52] V. Vinod, R. Sashidhar, Food Chem. 116 (3) (2009) 686–692.
[53] L. Wang, D. Xiang, C. Li, W. Zhang, X. Bai, J. Mol. Liq. 345 (2022) 117009.
[54] X. Zhou, Y. Yang, J. Ma, K. Zhang, J. Song, L. Wang, B. Liu, J. Zhang, Z. Lu, Y. Tang, Nucl. Eng. Des. 360 (2020) 110527.
[55] P.P. Magampa, N. Manyala, W.W. Focke, J. Nucl. Mater. 436 (1–3) (2013) 76–83.
[56] S. Jaiser, N. Sanchez Salach, M. Baunach, P. Scharfer, W. Schabel, Drying Technol. 35 (15) (2017) 1807–1817.
[57] S.G. Patnaik, R. Vedarajan, N. Matsumi, J. Mater. Chem. A 5 (34) (2017) 17909–17919.
[58] Z. Ding, X. Li, T. Wei, Z. Yin, X. Li, Electrochim. Acta 196 (2016) 622–628.
[59] M. Gao, N. Liu, Y. Chen, Y. Guan, W. Wang, H. Zhang, F. Wang, Y. Huang, Chem. Commun. 51 (60) (2015) 12118–12121.
[60] X. Rao, Y. Lou, J. Chen, H. Lu, B. Cheng, W. Wang, H. Fang, H. Li, S. Zhong, Front. Energy Res. 8 (2020) 3.
[61] K. Lee, S. Lim, N. Go, J. Kim, J. Mun, T.-H. Kim, Sci. Rep. 8 (1) (2018) 11322.
[62] C. Ma, Y. Zhao, J. Li, Y. Song, J. Shi, Q. Guo, L. Liu, Carbon 64 (2013) 553–556.